Polydisperse Tube Diameters Compromise Multiple Open Tubular Chromatography

D. K. Schisla, Hongbing Ding, P. W. Carr, and E. L. Cussler
Depts. of Chemical Engineering, Materials Science, and Chemistry, University of Minnesota, Minneapolis, MN 55455

This article demonstrates that even 1% polydispersity in hollow-fiber diameters can increase plate heights by as much as an order of magnitude. The demonstration includes an analytical extension of the Taylor-Aris and the Golay dispersion theories, a numerical solution using the measured polydisperity, and successful predictions of the performance of different hollow-fiber systems over a range of flow rates. All these results show that the effect of polydispersity can dominate column performance, especially in the region where the column efficiency is optimal.

Introduction

Large-scale open tubular column chromatography promises higher productivity and more theoretical plates than does particle bed chromatography. The higher productivity is a consequence of lower pressure drop per column length, which results from dramatically reduced form drag. The greater number of theoretical plates is a consequence of more uniform geometry and is possible even when the surface area per volume in tubes is smaller than in particle beds.

These promises have been at least partially realized for open tubular gas chromatography. For liquids, large-scale open tubular chromatography has been less successful, even in the face of substantial effort. At a small scale, low pressure drops and a few million plates can be achieved with appropriate injection and analytical devices. However, efforts to increase this scale from nanoliters to liters have had limited success. Most of these systems sensibly use arrays of channels operating in parallel. Arrays made of solid fibers have been developed industrially, but have given disappointing plate heights. Arrays made with hollow fibers have performed more closely to expectation, but these expectations have been modest because fiber diameters have been 100 μm or larger (Ding et al., 1989; Schisla, 1990; Ding, 1992).

We believe that the disappointing performance of these arrays of many channels is due partly to the polydispersity of the channel size. To test this belief, we first extend the usual analysis of open tubular chromatography to polydisperse arrays of hollow fibers. In this extension, we build on earlier studies of Taylor (1953, 1954), Golay (1958), Turner (1958), and Aris (1959a), but we stress results which are easy to use. We then verify this extended analysis with numerical studies and new experiments of multiple hollow-fiber liquid chromatography. Thus, this article supplies both an explanation for the compromised performance of this chromatographic method and a standard to judge when this method will be improved.

Theory

Our analysis of multiple open tubular chromatography is based on the behavior of a single cylindrical capillary. In such a capillary, the exit concentration c_1 of a solute pulse is given by the equation (Golay, 1958):

$$c_1 = \frac{M/(\pi R^2 L)}{\sqrt{2\pi}(\sigma/t_R)} e^{-(t-t_R)^2/2\sigma^2} \tag{1}$$

in which M is the total amount of solute injected, R is the capillary radius, L is its length, and t is the time. The average residence time in the column t_R is:

$$t_R = \frac{L}{v}(1+k') \tag{2}$$

where v is the average mobile-phase velocity in the single capillary and k' is the capacity factor. The variance of the residence time σ^2 is given by:

$$\sigma^2 = \frac{2DL}{v^3}(1+k')^2 + \frac{R^2 L}{24Dv}[1+6k'+11(k')^2] + \frac{2\delta^2 k' L}{3D'v} \tag{3}$$

The first term on the righthand side of this equation is due to

axial diffusion and so varies directly with the diffusion coefficient in the mobile phase D. The second term describes Taylor-Aris dispersion, a combination of radial diffusion and laminar axial convection. The third term on the righthand side results from diffusion in the stationary phase and so varies with the thickness of this phase δ and the solute's diffusion coefficient in this phase D'. Equation 3 is often written as a reduced plate height h, an alternative measure of dispersion:

$$h=\frac{L\sigma^2}{2Rt_R^2}$$
$$=\frac{2}{u}+\left[\frac{1+6k'+11(k')^2}{96(1+k')^2}\right]u+\left[\frac{1}{6}\frac{(k')}{(1+k')^2}\frac{D}{D'}\left(\frac{\delta}{R}\right)^2\right]u \quad (4)$$

where $u(=2Rv/D)$ is called the reduced velocity in chemistry and the Peclet number in engineering. The three terms in the righthand side of Eq. 4 have the same physical origins as the same three terms in Eq. 3.

The variance σ^2 or the reduced plate height h is a critical variable in describing the performance of any chromatographic column. As a result, this variable is often calculated not from the Gaussian curve given in Eq. 1, but as the second moment of the eluted concentration profile:

$$\sigma^2=\frac{\int_0^\infty (t-t_R)^2\pi R^2 v c_1 dt}{\int_0^\infty \pi R^2 v c_1 dt} \quad (5)$$

This expression allows easy calculation of the variance from experimental data.

We now extend the analysis for this single cylindrical capillary to an array of parallel capillaries. We expect that variations in capillary diameter will be more significant than variations in capillary length, so we assume a single fixed length L. We then define a normalized distribution function of capillary radii, $g(R)$, such that:

$$1=\int_0^\infty g(R)dR \quad (6)$$

Note that $g(R)$ has dimensions of reciprocal length. We can use this function to find average properties of the array. For example, the average radius is:

$$\langle R\rangle=\int_0^\infty Rg(R)dR \quad (7)$$

The average velocity over the array of capillaries $\langle v\rangle$ is more subtle:

$$\langle v\rangle=\frac{\int_0^\infty \pi R^2 v(R)g(R)dR}{\int_0^\infty \pi R^2 g(R)dR} \quad (8)$$

Because we have laminar flow, the velocity averaged over a single fiber is (Bird et al., 1960):

$$v(R)=\frac{\Delta p R^2}{8\mu L} \quad (9)$$

where Δp is the pressure drop and μ is the mobile-phase viscosity. Finally, we define the average variance $\langle\sigma^2\rangle$ of the array of capillaries:

$$\langle\sigma^2\rangle=\frac{\int_0^\infty\int_0^\infty (t-t_R(R))\pi R^2 v(R)c_1(R,t)g(R)dRdt}{\int_0^\infty\int_0^\infty \pi R^2 v(R)c_1(R,t)g(R)dRdt} \quad (10)$$

This average is the desired result of our analysis.

We can find this average variance by three routes. First, we can experimentally measure the distribution of radii $g(R)$, and then numerically integrate Eq. 10 and its supporting relations, Eqs. 1-3 and 9. This calculation is straightforward and will be performed in the results section for some special cases. The method, however, is tedious and clumsy, and will rarely be used on a routine basis.

The second route to calculating the average radius would build on the pioneering studies of Turner (1958) and of Aris (1959b), who explored the dispersion in packed beds of parallel channels. The work of these authors suggests exact integrals and gives methods by which these can be calculated. Unfortunately, this second route is mathematically elaborate. Moreover, because Turner and Aris did not consider any effects of the stationary phase, any calculation useful chromatographically would require extensive development. We have chosen not to explore this second route.

The third route to finding $\langle\sigma^2\rangle$, which we stress here, assumes that distribution of fiber diameters is Gaussian. This form can then be used to evaluate the double integral in Eq. 10. To keep this integration especially simple, we also will expand the integral as a Taylor series in deviations from the average radius. Thus, our integration yields a power series in this deviation of radii and will be accurate only when this deviation is small. We expect that capillary arrays with packed beds must show only small deviations to be competitive, so this assumption is appropriate.

To explore this third route, we assume that the distribution of capillary radii is:

$$g(R)=\frac{1}{\sqrt{2\pi}\sigma_R}e^{-\frac{(R-\langle R\rangle)^2}{2\sigma_R^2}} \quad (11)$$

where σ_R^2 is the variance of the capillary radii, not the temporal variance of the solute concentration given in Eq. 3. We will find it convenient to rewrite this distribution in dimensionless terms:

$$g(R)=\frac{g(\epsilon)}{\langle R\rangle}=\frac{1}{\sqrt{2\pi}\langle R\rangle\epsilon_0}e^{-\frac{\epsilon^2}{2\epsilon_0^2}} \quad (12)$$

where

$$\epsilon \equiv (R - \langle R \rangle)/\langle R \rangle \tag{13}$$

and

$$\epsilon_0 \equiv \sigma_R/\langle R \rangle \tag{14}$$

We expect both ϵ and ϵ_0 to be small relative to one. We also assume that the thickness of the stationary phase is proportional to the tube diameter. As a result, the capacity factor k' is independent of radius R and can be taken equal to that of a fiber of average radius $\langle R \rangle$. This assumption is not the only sensible one; for example, we could assume that the thickness of the stationary phase is constant, independent of the capillary radius R. Doing so leads to somewhat more complicated final equations, but the numerical predictions of these equations are much like those with the above assumption (Ding, 1992).

We can now use Eq. 12 to calculate the various average quantities in terms of the dimensionless radial variance ϵ_0^2. Reassuringly, combination and integration of Eqs. 7 and 12 show that the average radius is $\langle R \rangle$. Combination of Eqs. 8 and 12 gives:

$$\langle v \rangle = \left(\frac{\Delta p \langle R \rangle^2}{8\mu L}\right)\left\{\frac{1 + 6\epsilon_0^2 + 3\epsilon_0^4}{1 + \epsilon_0^2}\right\} \tag{15}$$

The quantity in parentheses in Eq. 15 is the average velocity expected from the average radius; the quantity in braces is the ratio of the true average velocity to that expected from the average radius. In a similar way, the residence time is now:

$$\langle t_R \rangle = \frac{L}{\langle v \rangle}(1 + \langle k \rangle) \tag{16}$$

where

$$\langle k \rangle = \frac{k'}{1 + \epsilon_0^2} \tag{17}$$

Finally and most importantly, the average variance defined by Eq. 10 can be calculated by combination and integration of Eqs. 1-3, 9, 10 and 12. The result is most easily written as:

$$\langle \sigma^2 \rangle = \langle \sigma^2 \rangle_{\text{axial diffusion}} + \langle \sigma^2 \rangle_{\text{Taylor-Aris dispersion}} + \langle \sigma^2 \rangle_{\text{stationary phase}} + \langle \sigma^2 \rangle_{\text{polydispersity}} \tag{18}$$

where the subscripts on the four terms on the righthand side stress the physical origin of each. More specifically,

$$\langle \sigma^2 \rangle_{\text{axial diffusion}} = \left(\frac{2DL}{\langle v \rangle^3}[1 + \langle k \rangle^2]\right)\{1 + 12\epsilon_0^2 + \ldots\} \tag{19}$$

The quantity in parentheses in Eq. 19 is close to the axial diffusion term in Eq. 3; the quantity in braces is the correction due to the capillary polydispersity. Similarly,

$$\langle \sigma^2 \rangle_{\text{Taylor-Aris dispersion}} = \left(\frac{\langle R \rangle^2 L}{24D\langle v \rangle}[1 + 6\langle k \rangle + 11\langle k \rangle^2]\right)\{1 + 5\epsilon_0^2 + \ldots\} \tag{20}$$

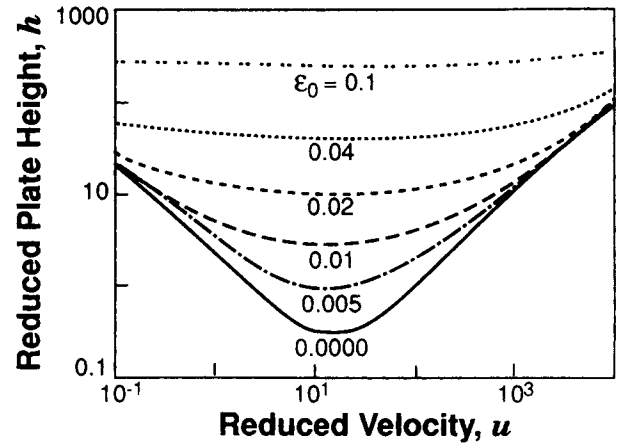

Figure 1. Effect of polydispersity on reduced plate heights.

The solid line is the usual result for a single capillary. The dotted lines are the greater reduced heights in multiple polydisperse capillaries with a reduced variance of ϵ_0^2 (cf. Eqs. 12-14).

$$\langle \sigma \rangle^2_{\text{stationary phase}} = \left(\frac{2\delta^2 L\langle k \rangle}{D\langle v \rangle}\right)\{1 + 5\epsilon_0^2 + \ldots\} \tag{21}$$

and

$$\langle \sigma^2 \rangle_{\text{polydispersity}} = \left(\frac{L}{\langle v \rangle}\right)^2 \{(4 + 12\langle k \rangle + 9\langle k \rangle^2)\epsilon_0^2 + \ldots\} \tag{22}$$

When ϵ_0^2 is zero, the capillaries are monodisperse, and Eqs. 18-22 collapse to Eq. 3.

The results of the analysis given above show that polydispersity increases the variance of a peak eluted from multiple open tubular chromatography. More bluntly, parallel columns of even slightly different radii give observably broader peaks. But, however clear the outlines of the derivation above are, their algebra still can obscure the physical size of the effects involved. How much broader are the peaks?

One easy way to see this is to calculate the peak's variance or the reduced plate height as a function of reduced velocity and the variance of the radii. One such plot for a species not retained in the column is given in Figure 1. It shows that the effects of polydispersity can be very important indeed. For example, imagine that we are operating at a reduced velocity of 10, near the minimum in the reduced plate height. Imagine also that our capillaries are polydisperse, with an apparently minor standard deviation of 1%. In other words, ϵ_0 is 0.01; the variance ϵ_0^2 is 10^{-4}. It looks minor indeed. But the results in Figure 1 show that the reduced plate height is increased more than ten times, dramatically reducing the performance of the open tubular array.

Thus, fiber polydispersity is a potentially devastating effect. As Figure 1 shows, it is especially devastating when columns are operated near the optimum reduced velocity; it is less compromising when the column is operated away from this minimum. For example, in the above case with a 1% standard deviation, the reduced plate height increases around 10% if the reduced velocity is 100 times its optimum value.

We must stress our present conclusion that the importance

of capillary polydispersity is based on theory only. The foundations of this theory, which include the Golay equation and a Gaussian distribution of fiber diameters, seem sensible and secure. Still, our arguments will be more convincing if they can be buttressed with experiments and a more precise numerical solution to the polydispersity problem. We turn to these experiments and the numerical model in the next sections.

Experimental Studies

The analytical solution derived above can be used to estimate the performance of a multiple capillary chromatograph. However, four assumptions are key to its development: 1. the fibers' diameters are to be represented as a Gaussian distribution; 2. the band broadening in a single capillary is described by Golay's theory for a thin, retentive layer; 3. the solute pulse is evenly distributed among the fibers; and 4. the capacity factor is independent of tube radius (Ding, 1992). We can test these assumptions both by numerical simulations and by physical experiments. The methods for both tests are described in this section.

Numerical simulations

The numerical simulations are based on a model which uses any functional form for the fiber diameters and Aris' (1956, 1959a) solution for a single capillary (Schisla, 1990). Aris' solution takes into account the curvature of the stationary phase, making no assumptions about film thickness. The variance in this case is:

$$\sigma^2=\frac{2DL}{v^3}(1+k')^2 + \frac{L}{v}\left[\frac{R^2}{24D}(1+6k'+11k'^2)+\frac{k'f(p)(2R\delta+\delta^2)}{D'}\right] \quad (23)$$

where $p=(R+\delta)/R$ and

$$f(p)=\frac{\left[\frac{2p^4\ln p^2}{p^2-1}-(3p^2-1)\right]}{8(p^2-1)}. \quad (24)$$

The function $f(p)$, which represents the curvature of the film, becomes important when the stationary-phase thickness is a significant fraction of the capillary radius, which is the case for the hollow fibers used here (Schisla and Carr, 1990). Like the analytical solution, the numerical model assumes that the pressure drop is the same over all the fibers, so that the solute pulse in each fiber is proportional to the fraction of volumetric flow going through that fiber. The concentration profile is then obtained by summing over all the single capillary concentration profiles at the outlet with each capillary, weighted by the fraction of volumetric flow going through each fiber. Moments are then calculated by integration. Such a calculation requires estimates of the diffusion coefficient in the mobile and stationary phase and of the capacity factor. The diffusion coefficient in the mobile phase was estimated using the Wilke-Chang correlation (Wilke and Chang, 1955; Cussler, 1984). The stationary-phase diffusion coefficient was determined from (Aris, 1975):

$$D'=D^0\epsilon_m/\tau \quad (25)$$

where D^0 is the diffusion coefficient in the bulk phase, ϵ_m is the porosity of the membrane, and τ is the tortuosity, estimated as two (Kiani et al., 1984). The diffusion coefficient of the solute through the gel phase was fitted from the experimental data of the variance using the numerical model. The capacity factors and partition coefficients were obtained by regression of the experimental residence time data. Details are given elsewhere (Schisla, 1990).

Module experiments

Hollow-fiber modules were fabricated as previously described from microporous polypropylene fibers (Celgard X10, Hoechst-Celanese) (Ding et al., 1989; Schisla, 1990). These fibers have nominal inside diameters of 100 and 240 μm, and a 25-μm wall thickness. Two different stationary phases were used. One, a 50/50 vol. % mixture of trioctylphosphate and dodecanol, was easily impregnated into the fibers' pores. The second was a polyvinylalcohol gel, cross-linked within the pores, as described elsewhere (Schisla, 1990). An array of glass channels from Schott Optical was also tested (Walter Sigmund, Schott Fiber Optics, Southbridge, MA). This array is made by carefully drawing a hollow glass tube, doubling the resulting tube back on itself, drawing again, doubling back again, and so on. Similar arrays with still smaller capillary diameters can be made by drawing a glass tube filled with an etchable glass rod and then etching out the etchable rod to make the array (Tonucci et al., 1992). The glass channels form a hexagonal array with inside diameters of 15.6 μm as determined by scanning electron microscopy. The glass channels were mounted in a stainless steel tube with epoxy, and the ends were carefully cut with a diamond saw (Ding, 1992). The glass columns were tested without any modification to the surface, that is, with unretained solutes.

The polydisperse fiber diameters and wall thicknesses of the polypropylene hollow fibers were measured with an optical microscope at 100 times magnification. The fibers have six characteristic diameters, each consistent to within 1%. Therefore, the distribution of fiber diameters were estimated using six equally represented groups. The nominal 100-μm-diameter fibers were estimated to be 99, 100, 102, 104 (twice) and 106 μm. The nominal 240-μm fibers were estimated to have a distribution of 232, 239, 241, 243, 244 and 246 μm. The fiber wall thickness was not observed to deviate significantly from the 25 μm reported by the manufacturer. The standard deviation of the Gaussian diameter distribution ϵ_0 is computed directly from the radii measured using either Eq. 11 or the definition of standard deviation for a population of N data:

$$\langle R\rangle=\sum_{i=1}^{N}R_i/N \quad (26)$$

and

$$\epsilon_0^2=\sigma_R^2/\langle R\rangle^2 = \sum_{i=1}^{N}(R_i-\langle R\rangle)^2/[\langle R\rangle^2(N-1)] \quad (27)$$

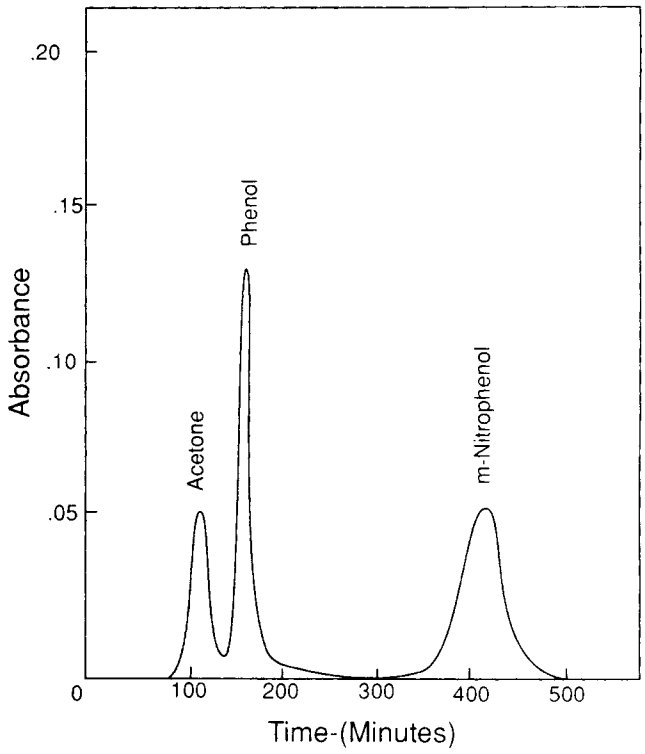

Figure 2. Small solute separation with a gel stationary phase.

The module contains 120 fibers with 100-μm ID and 50-cm length. The absorbance units are arbitrary.

Values of ϵ_0 of 0.023 and 0.021 were obtained for the 100- and 240-μm-diameter fibers, respectively. The diameters of the glass fibers were measured from an SEM photograph of the array's end. Hundreds of diameters were measured giving a ϵ_0 value of 0.0085 for the glass array.

The hollow-fiber and glass-capillary columns were installed in the experimental apparatus described in detail elsewhere (Ding et al., 1989; Schisla, 1990; Ding, 1992). A Hewlett-Packard Integrator (model 3396A) was used in the data analysis for the glass-column and gel stationary-phase experiments, while a Macintosh data acquisition system was used for the liquid stationary phase runs. Distilled water was used as the mobile phase in the hollow-fiber systems; *n*-hexane was used in the glass capillary system. All chemicals were reagent grade and were used as received. The solute was injected as a dilute solution of 10-20 μL.

Results

The previous sections showed how chromatography in multiple tubular channels is affected by the polydispersity of the channels. The effect of the polydispersity can be approximately predicted using an analytical solution based on the assumption of a narrow Gaussian distribution of diameters. Predicting the effect from this analytical solution is easy. The effect of polydispersity can also be predicted by numerically adding the effects of individual fibers of measured diameters to obtain results unbridled by the Gaussian assumption. Predicting the effect in the numerical way is tedious.

In this section, we begin by showing that the easy, approximate analytical predictions of polydispersity are equivalent to the tedious numerical ones. We then show when the effects of polydispersity are most significant. Typical peaks found in these experiments are shown in Figure 2; typical data inferred from these peaks are shown in Figure 3. The experimental data shown are for the solutes, methyl butanone and phenol, with the liquid and gel stationary phases, respectively. The liquid stationary column contained 420 fibers, 100 μm in diameter and 60 cm in length. The gel stationary-phase column contained 120 fibers, 240 μm in diameter and 50 cm in length.

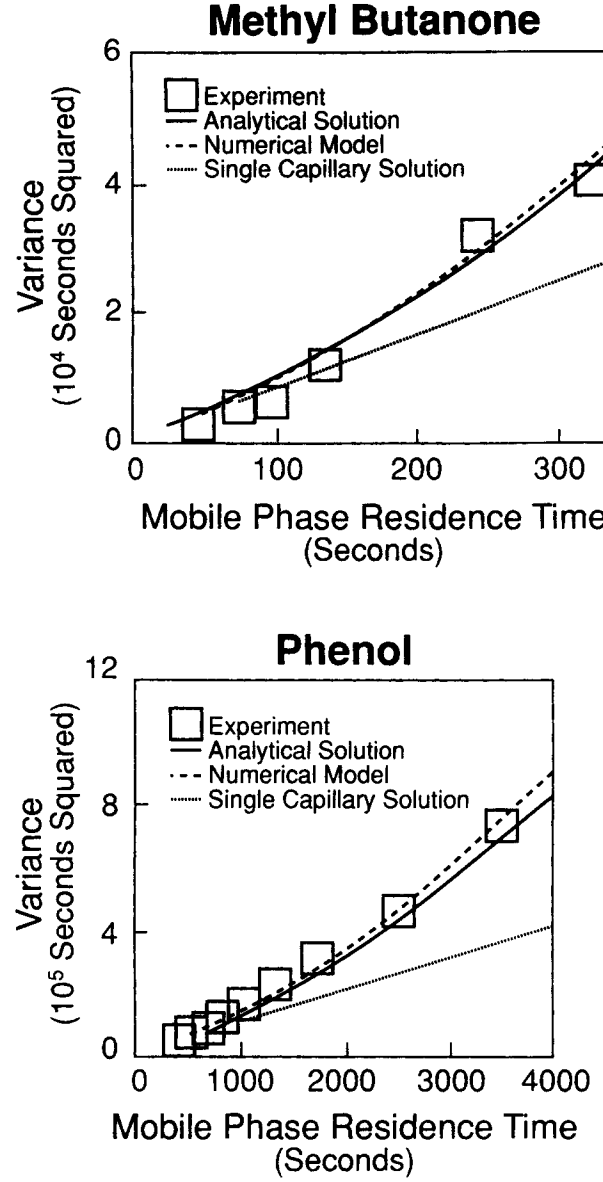

Figure 3. Effect of polydispersity on peak variance.

Methyl butanone was the solute in 100-μm liquid, stationary-phase column with $\epsilon_0 = 0.023$; phenol was the solute in 240-μm gel, stationary-phase column with $\epsilon_0 = 0.021$.

Figure 3 shows that the analytical solution and numerical model are virtually identical and are in good agreement with the experimental data. The variance approaches the single capillary solution at short mobile-phase residence times, that is, at high velocities, but it increases dramatically above this as

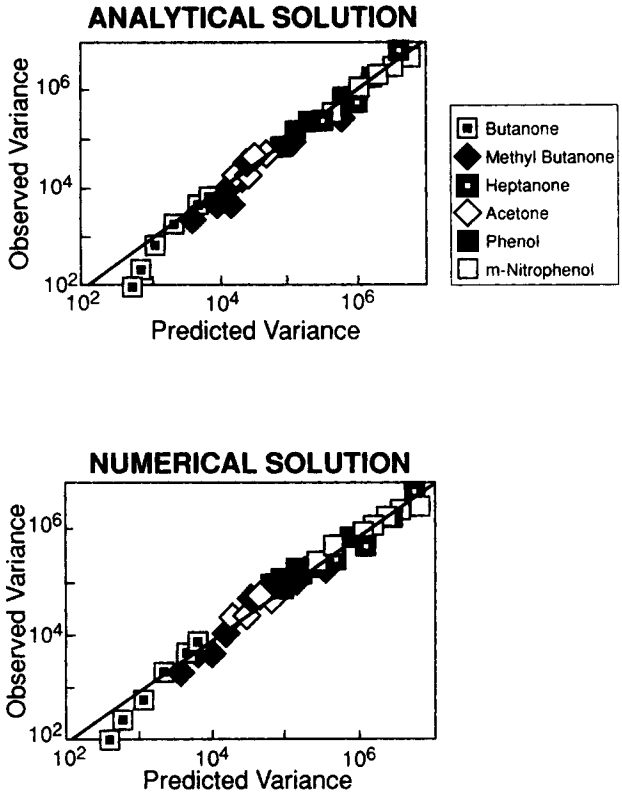

Figure 4. Evaluation of analytically and numerically computed variance.

Solutes, butanone, methyl butanone, and heptanone were tested on a 100-μm-ID liquid stationary-phase column with $\epsilon_0 = 0.023$; solutes acetone, phenol, *m*-nitrophenol were tested on a 240-μm-ID gel stationary-phase column with $\epsilon_0 = 0.021$.

the velocity is reduced. At the longest residence times observed, the polydispersity accounts for about 30% of the total peak width in the case of methyl butanone and about 60% in the case of the phenol.

These results for methyl butanone and phenol are typical of those obtained in our experiments, as shown in Figure 4 for a wide variety of solutes. Both the analytical and the numerical

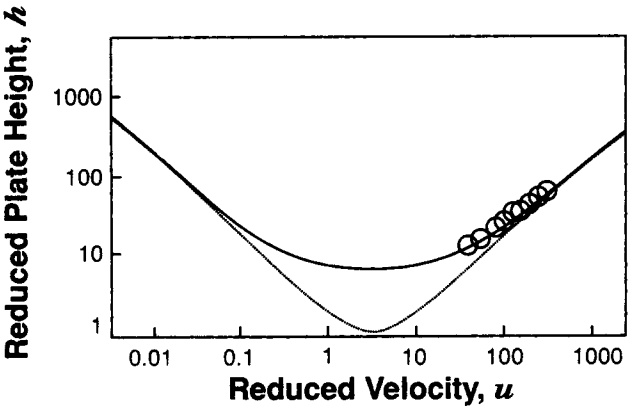

Figure 5. Effect of polydispersity on column efficiency.

The circles, experimental values for phenol chromatography in hollow fibers with ϵ_0 of 0.021 are close to the solid line predicted from Eq. 18. The dotted line is the limit without polydispersity (Eq. 3).

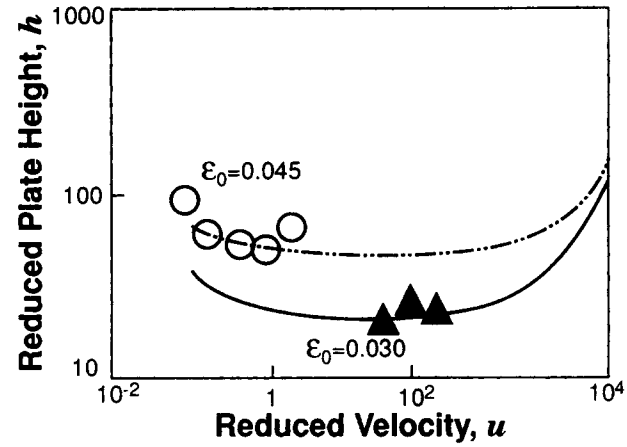

Figure 6. Reduced plate heights for multiple channels made of glass.

The triangles refer to the open channels, 15.6 μm in diameter, made in glass arrays. The open circles are for the spaces around solid glass fibers which are 18 μm in diameter (Czok and Guichon, 1990).

models are in excellent agreement with the experimental data. The agreement is accurate over a range of velocities and of capacity factors, which were 0.93, 3.5, and 58 for the liquid column, and 1.85, 4.03, and 13.2 for the gel column. The only discrepancy between the predicted and observed behavior occurs for the slightly retained methyl butanone at mobile-phase residence times below 50 seconds.

At the same time, we should stress that these successes are not the most stringent tests which we could make on these systems. Our apparatus permitted measurements at relatively high reduced velocities. This is illustrated by the phenol results in Figure 5. Under the conditions we studied, the reduced plate height can be about twice that expected from the theory of a single capillary. This is a consequence of a standard deviation ϵ_0 of 0.021 measured for the hollow fibers used in this module. This result, however, is for a reduced velocity more than ten times that predicted to give the minimum plate height. Had we used the lower reduced velocity, our plate height would have been ten times larger than the minimum value, an increase of 1,000% caused by a polydispersity of 2%. Still, few capillaries are ever operated at such low flows.

Similar results are obtained for both arrays of glass channels and for solid glass fibers, as shown in Figure 6. The glass array contains 10,413 capillaries with nominal tube diameters of 15.6 μm and a length of 6.5 cm. The reduced plate heights obtained with the arrays are smaller than those observed for columns packed with 18 μm aligned solid fibers, which produce nominal 3-μm capillaries (Czok and Guiochon, 1990). With such small capillaries, the solid fiber column should be more efficient; its reduced efficiency is probably due to polydispersity generated during column packing.

Discussion

The goal of this article is to show that multiple capillary chromatography is compromised seriously by polydisperse capillaries and that this compromise can be successfully predicted by either analytical theory or numerical calculation. We now want to evaluate our success in reaching this goal.

Table 1. Estimation of Phenomena Contributing to Band Broadening

System Dia. and k'	L/v s	Percent Contribution to the Variance: Axial Diff.	Mobile-Phase Dispersion	Stationary-Phase Diffusion	Polydispersity in Capillary Diameter
15.6 μm	0.3_2	0	85	0	15
$k'=0$*	1.1	0	64	0	36
	3.2	1	37	0	62
	8.0	2	19	0	79
100 μm	100	0	30	60	10
$k'=4.2$**	250	0	25	49	26
	400	0	22	45	33
240 μm	6,000	0	23	45	32
$k'=1.8$†	18,000	0	17	33	50
	36,000	0	14	27	59

* Plain glass surface; solute—benzene
** Liquid stationary phase; solute—2-methyl-3-butanone
† Gel stationary phase; solute—phenol

Our experiments with hollow-fiber chromatography show close agreement between experiment and theory for a wide variety of chemical systems. We are especially pleased that our approximate analytical model agrees so closely with our numerical calculations. Differences between the experiments and analytical prediction are within the error of the parameters used in the model, that is, the diffusion coefficients and the radial variance ϵ_0^2. The analytical solution is for all purposes equivalent to the numerical model. It should be used exclusively for predictions because it is so straightforward.

Deviations between experiments and the analytical model in the hollow-fiber systems are observed at short mobile-phase residence times. This may occur because the Taylor-Aris-Golay single capillary solution breaks down at these conditions. It satisfies the assumption made for a smooth, unretentive capillary wall that the time the pulse takes to travel through the column is long compared to the diffusion of the solute over the cross-section of the capillary. When a retentive layer is present, however, we make a similar assumption implicitly for the stationary phase: the solute must also be given ample time to equilibrate with the stationary phase before it is removed by the mobile phase. For slightly retained species at high flow rates, this assumption is not satisfied. As a result, the variance in each capillary is overestimated. Because most chromatographic systems operate under conditions where the assumption is appropriate, our analytical solution will usually be accurate.

The analytical solution shows how dramatically polydispersity can affect the efficiency of multiple capillary chromatographs. The contribution of the various band broadening phenomena is summarized in Table 1. The first column describes the multiple capillary column, and the second gives characteristic values of the time (L/v). The remaining columns give the contributions to the variance that form the capillary diameter. For the conditions given, this contribution is often 30% of the total and can be 80% of the total.

Moreover, the results in Table 1 are for relatively *favorable* conditions. In other circumstances, the plate height can be increased by an order of magnitude at its minimum (cf. Figure 1). This supports previous work on the importance of diameter matching in analytical chromatography applications (Meyer et al., 1983). The effect of diameter matching may not be as important in preparative applications, as the maximum throughput occurs often at high flow rates, away from the minimum plate height (Knox and Pyper, 1986). Preparative chromatography in multiple capillary columns is addressed in more detail elsewhere (Ding and Cussler, 1990; Schisla et al., 1992).

The success of our theory and experiments raise two other questions. First, why is the separation so sensitive to minor polydispersity in tube diameters? Second, how can this polydispersity effect be reduced? While we are unsure of either answer, we want to explore these points here.

To see why radial polydispersity has such a major effect, imagine a chromatography column comprising just two tubes. The tubes are of equal length, but one has an internal diameter twice the other. We might casually assert that the appropriate diameter used to estimate the elution of a solute pulse should be the arithmetic average of the two tubes. We would then be surprised that the performance of this two-tube column is much poorer than our estimates.

We can understand why these estimates would be in error by considering the flow through the two tubes more carefully. Because the flow in both tubes would be laminar, the larger tube would carry 16 times the flow of the smaller one. The actual two tubes would carry three times more flow than two tubes of the average diameter. Moreover, fluid in this larger tube would have only one fourth the residence time and 16 times the Taylor-Aris dispersion. All these effects contribute to peak spreading and so exceed those expected from a simple increase in the average diameter.

The second question concerns how this polydispersity effect might be reduced. It is especially severe because it persists *over the entire length of the bed*: any fluid which enters the largest hollow fiber in multiple-fiber beds also leaves the bed from the same largest hollow fiber. In contrast, fluid moving past an unusually large particle in a packed bed will have its flow altered only for a few particle diameters.

The obvious way to reduce the effect of polydispersity is to cut our bed into short lengths, to rotate the lengths, and to glue the bed together again. This would accomplish much the same aim as distributor plates installed in a conventional packed tower. We believe that this idea would work. At the same time, we must remember that our original hope for multiple tubular beds was that they would show less form drag and hence less pressure drop than conventional packed beds. We are concerned that cutting our tubular beds into small segments will solve the polydispersity problem by resurrecting the large pressure drop.

Our analytical solution for multiple open tubular chromatography gives a simple means for evaluating the effect of polydispersity that was not previously available. While the hollow fibers are reproducible enough to describe quantitatively, their large radii make it difficult to realize adequate efficiencies for analytical applications. The glass fibers and arrays tested promise higher efficiencies as a result of small radii, but the radii are not sufficiently well-matched to compete with packed beds. The search for smaller capillaries with better reproducibility must continue.

Acknowledgment

This work was supported chiefly by Hoechst Celanese and by the

National Science Foundation (grant number CTS 91-23837). Other support came from DARPA 92-05112 and from General Mills. E. L. Cussler held the Amundson Professorship while on sabbatical leave at the Massachusetts Institute of Technology, where he was graciously welcomed.

Notation

c_i = solute concentration
d = capillary diameter, twice the average radius
D = diffusion coefficient in the mobile phase
D' = diffusion coefficient in the stationary phase
$g(\epsilon)$ = dimensionless distribution function
$g(R)$ = distribution function of capillary radii (Eq. 6)
h = reduced plate height (Eq. 4)
k' = capacity factor
$\langle k \rangle$ = average capacity factor (Eq. 17)
L = capillary length
M = total amount of solute injected (Eq. 1)
N = total number of fibers
p = dimensionless radius (Eq. 23)
R = radius of one capillary
$\langle R \rangle$ = average radius (Eq. 7)
t = time
t_R = residence time (Eq. 2)
$\langle t_R \rangle$ = average residence time
u = reduced velocity or Peclet number (Eq. 4)
v = mobile phase velocity
$\langle v \rangle$ = average velocity (Eq. 8)

Greek letters

δ = thickness of stationary phase
Δp = pressure drop in capillary
ϵ = dimensionless deviations from mean radius (Eq. 13)
ϵ_m = void fraction of the fiber wall (Eq. 25)
ϵ_0^2 = dimensionless variance (Eq. 14)
μ = viscosity of mobile phase
σ^2 = variance of residence times (Eq. 3)
σ_R^2 = variance of capillary radii (Eq. 11)
$\langle \sigma^2 \rangle$ = average variance of residence times (Eq. 10)
τ = tortuosity of the fiber wall (Eq. 25)

Literature Cited

Aris, R., "On the Dispersion of a Solute in a Fluid Flowing through a Tube," *Proc. Roy. Soc.*, London, **A235**, 67 (1956).
Aris, R., "On the Dispersion of a Solute by Diffusion, Convection and Exchange between Phases," *Proc. Roy. Soc.*, London, **A252**, 538 (1959a).
Aris, R., "Diffusion and Reaction in Flow Systems of Turner's Structures," *Chem. Eng. Sci.*, **10**, 80 (1959b).
Aris, R., *Mathematical Theory of Diffusion and Reaction in Permeable Catalysts*, Oxford Clarendon Press, London (1975).
Bird, R. B., W. E. Steward, and E. N. Lightfoot, *Transport Phenomena*, Wiley, New York (1960).
Cussler, E. L., *Diffusion: Mass Transfer in Fluid Systems*, Cambridge Press, Cambridge (1984).
Czok, M., and G. Guiochon, "Aligned Fiber Columns for Size-Exclusion Chromatography," *J. Chromatog.*, **506**, 303 (1990).
Ding, H., "Hollow Fiber Liquid Chromatography and Fractional Extraction," PhD Thesis, Univ. of Minnesota (1992).
Ding, H., M.-C. Yang, D. K. Schisla, and E. L. Cussler, "Hollow Fiber Liquid Chromatrography," *AIChE J.*, **38**(5), 814 (May, 1989).
Ding, H., and E. L. Cussler, "Overloaded Hollow Fiber Liquid Chromatography," *Biotechnol. Prog.*, **6**, 472 (1990).
Golay, M. J. E., "Theory of Gas Chromatography," *Gas Chromatography—1958*, D. H. Desty, ed., Buttersworth, London (1958).
Kiani, A., R. R. Bhave, and K. K. Sirkar, "Solvent Extraction with Immobilized Interfaces in a Microporous Hydrophobic Membrane," *J. of Mem. Sci.*, **20**, 125 (1984).
Knox, J. H., and H. M. Pyper, "Framework for Maximizing Throughput in Preparative Liquid Chromatography," *J. of Chromatogr.*, **363**, 1 (1986).
Meyer, R. F., P. B. Champlin, and R. A. Harwick, "Theory of Multicapillary Columns for HPLC," *J. Chromatogr. Sci.*, **21**, 433 (1983).
Schisla, D. K., "Hollow Fiber Liquid Chromatography," PhD Thesis, Univ. of Minnesota (1990).
Schisla, D. K., and P. W. Carr, "Limitations of the Assumption of Negligible Film Thickness in Capillary Chromatography," *Chromatographia*, **29**(11/12), 606 (1990).
Schisla, D. K., M. N. Smith, P. W. Carr, and E. L. Cussler, "Preparative Multiple Capillary Chromatography," *J. Chromatogr.*, submitted (1992).
Taylor, G., "Dispersion of Soluble Matter in Solvent Flowing Slowly through a Tube," *Proc. Roy. Soc.*, London, **A219**, 186 (1953).
Taylor, G., "The Dispersion of Matter in Turbulent Flow through a Pipe," *Proc. Roy. Soc.*, London, **A223**, 446 (1954a).
Taylor, G., "Conditions under which Dispersion of a Solute in a Stream of Solvent Can Be Used to Measure Molecular Diffusion," *Proc. Roy. Soc.*, London, **A225**, 473 (1954b).
Tonucci, R. J., B. L. Justus, A. J. Campillo, and C. E. Ford, "Nanochannel Array Glass," *Sci.*, 783 (1992).
Turner, G. A., "The Flow-Structure in Packed Beds—A Theoretical Investigation Utilizing Frequency Response," *Chem. Eng. Sci.*, **7**, 156 (1958).
Wilke, C. R., and P. C. Chang, "Correlation of Diffusion Coefficients in Dilute Solutions," *AIChE J.*, **1**, 264 (1955).

Manuscript received Sept. 11, 1992, and revision received Dec. 17, 1992.